PCCP

ROYAL SOCIETY OF CHEMISTRY

PAPER

View Article Online
View Journal | View Issue

Cite this: *Phys. Chem. Chem. Phys.*, 2026, **28**, 4668

Tunable solvent-induced gelation of dipeptide-based gelators: exploring the role of solvent and acid concentration

Henna Rahkola, Efstratios D. Sitsanidis, Romain Chevigny † and Maija Nissinen *

Received 2nd October 2025,
Accepted 19th January 2026

DOI: 10.1039/d5cp03810c

rsc.li/pccp

The tunability of the solvent-induced gelation mechanism using *tert*-butyl (*t*Bu) containing solvents and two *t*Bu-protected dipeptide precursor gelators (Boc-Phe-Phe-O*t*Bu – **1** and Boc-Leu-Phe-O*t*Bu – **2**) is reported. Gelation behaviour, network morphology, material stability, and gelators' structures can be adjusted by both the solvent type and acid concentration. While *tert*-butyl chloroacetate (*t*BuClOAc) enables rapid gelation, *tert*-butyl methyl ether (*t*BuOMe), acting as a solvent with two leaving groups, promotes the *in situ* formation of two different gelators and prolongs the gelation time. Gel-to-sol transition temperature ($T_{gel-sol}$), NMR, HR-MS, ATR-FTIR and TEM analyses revealed that both the solvent type and acid concentration influenced the precursor gelator-to-gelator conversion efficiency, as well as the secondary structure (β-sheet and helical-like motif) and morphology of the resulting gels. This study highlights the adaptability of solvent-induced gelation across different solvent environments. In addition, the findings demonstrate that the solvent type and acid loading are powerful tools for tuning the properties of peptide-based supramolecular organogels with potential applications in biomedical and materials science.

Introduction

Low-molecular-weight gelators (LMWGs) are a diverse and useful class of compounds that can self-assemble, forming, for example, supramolecular gels.[1–3] Particularly, amino acid- and peptide-based LMWGs have attracted attention due to their simple structures, biocompatibility, biodegradability, and natural abundance. Their chemical and physical properties can be easily modified by altering the amino acid sequence or utilising various functionalisation options, for example, by the addition of protective groups at the C- and N-termini. This further enhances their potential as gelator building blocks and for applications in various fields.[4,5] By controlling the gelator structure, the solvent, and the gelation conditions, the desired properties of the gels can be tuned to a considerable extent.

The self-assembly of gelator peptides is a spontaneous, thermodynamically and kinetically driven process based on the development of intermolecular non-covalent interactions,[6] such as π–π stacking, hydrogen bonding, van der Waals forces and electrostatic interactions.[2,3,7,8] Due to the weak and dynamic nature of these interactions, self-assembled structures (and their corresponding macroscopic materials) can be modified by altering several parameters, including pH, temperature, the presence of counterions, concentration, solvent type, and the type of gelation trigger.[9–11] By controlling the kinetic parameters (*e.g.*, heating/cooling rates, solvent exchange or evaporation rates, agitation-shear forces, and diffusion rates), inherently dynamic metastable materials can be created.[6]

Additionally, in dissipative self-assembled (DSA) systems, non-gelator precursor molecules are activated into gelators by external energy input (*e.g.*, light, enzymes, or chemical fuels), leading to their assembly into ordered structures. Upon energy depletion, inhibition or intentional deactivation, the formed structures collapse, and initial precursors are formed.[12–14] These chemically fuelled self-assembled systems are thermodynamically unfavourable and thus require a continuous external energy input to maintain their out-of-equilibrium state.[15,16] In contrast, in-equilibrium self-assembled systems form stable and permanent structures that do not require continuous energy input. Although they may pass through dynamic, non-equilibrium intermediate states during formation, they eventually reach a thermodynamically favourable structure. Systems as such can exhibit continuous internal interconversion of states; however, once the system has reached equilibrium (or a favourable thermodynamic state), the forward and reverse processes occur at equal rates and do not affect the system's balance and stability.[13,15]

Department of Chemistry, Nanoscience Center, University of Jyväskylä, P.O. Box 35, FI-40014 JYU, Finland. E-mail: maija.nissinen@jyu.fi
† Current address: Université de Lorraine, CNRS, IJL, F-54000 Nancy, France.

Transient supramolecular materials created by DSA have been extensively studied. Due to their limited lifetimes, such materials are attractive for applications in drug delivery platforms and self-abolishing systems.[17] Properties including viscoelasticity, thermoreversibility, and dynamic reversibility enable gels to perform unique functions such as self-healing, responsiveness to external stimuli, and tolerance/adaptability to environmental changes. These properties are important for applications in pharmaceuticals (*e.g.*, drug delivery), the food industry, and cosmetics.[8,18]

The solvent environment of the gel material can be, for example, water (hydrogels), an organic solvent (organogels), or a mixture of the two.[8] In general, solvents do not participate actively in the self-assembly of gelator molecules but are instead encapsulated within the resulting gel network. Nevertheless, the solvent may affect the properties of the material, and in this case, its role is as important as the structure of the gelator. In some cases, the solvent can initiate the gelation process (*e.g.*, solvent exchange-triggered gelation):[11,19] the gelator solution is diluted with a non-solvent, and a balance is sought between the solubility and aggregation of the gelator molecules.

Usually, different solvents affect the gelation outcome primarily due to changes in solubility or being unsuitable for gel formation. Consequently, gelator–gelator and gelator–solvent interactions have a fundamental impact on self-assembly *per se* and on the properties of the resulting macroscopic gel material.[20–24] Stable, in-equilibrium gels form when intermolecular interactions, solubility parameters, and the forces driving fibrillar aggregation are in a delicate balance.[22,24,25] Reduced solvent–gelator interactions promote fibrillar growth, resulting in thinner, more flexible, and entangled fibres, whereas stronger gelator–gelator interactions favour the formation of thicker and shorter fibres.[20,21] Fibres can further interact, leading to the formation of bundles and ribbons.[24] Thus, the gelation process can be tailored by solvent properties, such as polarity and the ability to form weak interactions, including hydrogen bonds and π–π interactions.[11,20,22,23,26]

The choice of solvent can alter gel properties, such as mechanical strength, thermoreversibility, and thermal stability.[8,18,19] The boiling and freezing points of organic solvents can also be used to control the operating temperature range of organogels. For instance, if high heat tolerance is required, using a solvent with a higher boiling point is sensible.[8,18] Conversely, low boiling points cause solvents to evaporate more readily from the gel matrix, leading to gel shrinkage. Although this may be unfavourable for mechanical durability and thermal stability, it can be advantageous in applications where solvent removal is required.[8] The solvent can also influence the system's morphology,[9,26] for example, solvent-induced morphological changes can be seen as a structural transition. Indeed, Li *et al.*[26] observed that a toluene-based organogel transforms from fibrous to microcrystalline morphology upon the addition of ethanol as a co-solvent.

Recently, we introduced the concept of solvent-induced gelation (Scheme 1), in which the solvent (*tert*-butyl acetate, *t*BuOAc) is chemically active and participates in the formation of supramolecular organogels from various di- and tripeptides.[27,28] This process occurs when the solvent and precursor gelators share the same protective group. Gelation proceeds through [regio]selective and irreversible deprotection of the *N*-Boc-protected peptide precursor gelator. Concurrently, *tert*-butyl (*t*Bu) ester at the *C*-terminus undergoes reversible deprotection in the presence of *t*BuOAc (primary solvent) and sulfuric acid (accelerator). This reaction pathway yields two activated gelators (**a** and **b**) that interconvert *via* a hydrolysis–esterification cycle, leading to the formation of an organogel. At the same time, hydrolysis of the primary solvent (*t*BuOAc) produces an alcohol (secondary solvent; *tert*-butyl alcohol, *t*BuOH), providing $t\text{Bu}^+$ cations in the system and simultaneously acting antagonistically toward gelation. As the *t*BuOH concentration increases over time, it induces a gel-to-sol transition, resulting in the gradual dissolution of the organogel.

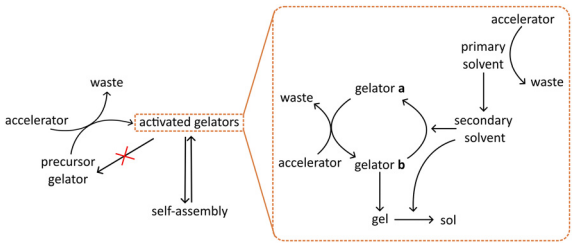

Scheme 1 Schematic representation of the previously reported solvent-induced gelation mechanism.

Based on previous research, we hypothesise that this gelation mechanism requires the presence of a common protective group in both the solvent and the precursor gelator.[28] To further explore the generalisability of this solvent-induced process, we investigated gelation in other *t*Bu-group-containing solvents and examined the effect of the amount of acid in these systems.

Results and discussion

Gel fabrication and gelation outcome

Based on our previous studies,[28] two dipeptide precursor gelators were selected for the solvent effect studies: Boc-Phe-Phe-O*t*Bu (**1**, gel system **I**) and Boc-Leu-Phe-O*t*Bu (**2**, gel system **II**) (Fig. 1). Four *t*Bu-group-containing solvents, *tert*-butyl chloroacetate (*t*BuClOAc), *tert*-butyl methyl ether (*t*BuOMe), *tert*-butyl acetoacetate (*t*BuAcAc), and *tert*-butyl formate (*t*BuOCHO), were chosen to investigate the gelation mechanism and self-assembly behaviour. Additionally, varying amounts of sulfuric acid (H_2SO_4; 1.0, 0.5 and 0.18 eq.) were used to assess the impact of acid concentration on gelation. This design allows us to examine whether shared functional motifs between the solvent and gelator contribute to the solvent-induced gelation, and how acid concentrations adjust the rate and extent of *in situ* precursor gelator activation, govern the efficiency of gel formation, and influence gel stability.

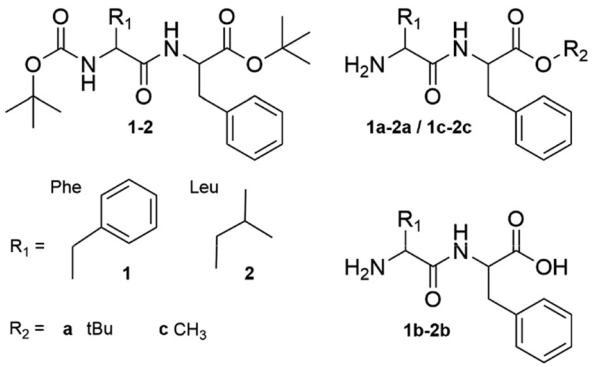

Fig. 1 The structures of precursor gelators **1** and **2**, monoprotected gelators **1a–1c** and **2a–2c** and deprotected gelators **1b–2b**.

All gel samples were prepared following the same protocol (experimental and S3.1, SI) using a constant precursor gelator concentration of 50 mM throughout the study. In addition, control gelation experiments were performed using the identified gelator molecules (**1a–c** and **2a–c**) alone to determine which of the *in situ* formed gelators can act as organogelators independently (Table S2, SI). The gelation outcome was evaluated using the vial-inversion method. Samples that "solidified" without any detectable free gravitational flow upon vial inversion were classified as self-supporting gels (SSGs). Those exhibiting "half-solidified" or weakly gel-like precipitate, along with flowable characteristics, were designated as partial gels (PGs), while samples showing no visible change were classified as solutions (Sol) (Table 1 and Table S1, SI). It is noteworthy that precursor gelator **1** is not soluble in *t*BuOMe, resulting in the formation of heterogeneous gels (Fig. S5, SI). However, upon heating these gels to their gel-to-sol phase transition temperature ($T_{gel-sol}$) and subsequently cooling to room temperature, homogeneous gels were obtained.

Gelation was not observed in *t*BuAcAc and *t*BuOCHO solvents under the tested conditions (Table S1, SI). Therefore, these were excluded from further study. In contrast, both gel systems **I** and **II** formed SSGs or PGs in *t*BuClOAc and *t*BuOMe, except for the sample with the highest amount of acid (1.0 eq.) in gel system **I** in *t*BuClOAc. The resulting organogels remained stable at room temperature for several months, except for gel system **II** in *t*BuClOAc and 1.0 eq. of acid, which reverted to a sol within two days after gelation. A similar transient behaviour was observed in our previous studies.[27,28] To evaluate whether the transient property of this gel system is caused by the formation of sufficient *t*BuOH to dissolve the gel system, the effect of *t*BuOH was tested on the highest-equivalent gel systems (S3.2, SI). After material formation, *t*BuOH (500 μL) was added on top of the materials. Here, it was found that precursor gelator **2**-based systems dissolved within 1 day, whereas precursor gelator **1**-based systems did not dissolve completely with the same amount of *t*BuOH, but required additional *t*BuOH (500 μL) to dissolve. This indicates that precursor gelator **2**-based systems are more susceptible to *t*BuOH than precursor gelator **1**-based systems, which partly explains why only gel system **II** in *t*BuClOAc with 1.0 eq. of acid exhibited transient behaviour.

In *t*BuClOAc, all gels formed within one day, regardless of the precursor gelator or acid concentration. In contrast, gelation in *t*BuOMe was significantly slower than in *t*BuClOAc and the previously reported *t*BuOAc,[28] with gelation times ranging from 5 to 14 days for both gel systems **I** and **II**. The amount of acid also influenced the gelation behaviour. Lower acid concentrations led to longer gelation times and outcomes ranging from SSGs to PGs. As the acid effect was particularly pronounced for gel system **II** in *t*BuOMe, higher acid equivalents (1.5 and 2.0 eq.) were tested, both of which produced SSGs (Fig. S5, SI) and reduced the gelation time to 4 days. These results demonstrate that both the solvent type and the acid concentration can be used to adjust gelation time and outcome.

The difference in gelation behaviour can be explained by the pH of the samples, which was assessed by three parallel pH measurements of solvent and precursor gelator mixtures (Table S3, SI). The data show that the initial pH (before acid addition) of the *t*BuClOAc mixtures is lower than that of the *t*BuOMe mixtures for both precursor gelators **1** and **2**. Therefore, the same amount of acid affects the two systems differently due to these distinct starting conditions, leading to a significantly lower final pH in *t*BuClOAc mixtures. This is reflected in the final gelation results, which show that SSGs form in *t*BuClOAc with lower acid amounts than in *t*BuOMe, and the gelation process occurs more rapidly.

The gels' $T_{gel-sol}$ were measured by controlled heating of the gels (in triplicate) and assessed by the vial inversion method to observe the phase changes (S3.4, SI). The measurements confirmed that the organogels are thermoreversible, as they transitioned to the sol state upon slow heating and reformed upon cooling to room temperature.

The solvent was found to affect the $T_{gel-sol}$ values (Table 1): slightly higher transition temperatures were observed in *t*BuOMe

Table 1 Gelation outcome and $T_{gel-sol}$ of gels

Precursor gelator	Acid (eq.)	*t*BuClOAc	$T_{gel-sol}$ (°C)	*t*BuOMe	$T_{gel-sol}$ (°C)
Boc-Phe-Phe-O*t*Bu (**1**)	1.0	Sol	—	SSG, transparent/opaque	55–60
	0.5	SSG, opaque	45–50	SSG, transparent/opaque	60–65
	0.18	SSG, opaque	55–60	SSG, transparent/opaque	60–65
Boc-Leu-Phe-O*t*Bu (**2**)	1.0	SSG, opaque[b]	40–45	SSG, transparent	55–60
	0.5	SSG, transparent	50–55	SSG/PG, transparent	60–65[a]
	0.18	SSG, transparent	55–60	PG, transparent	60–65[a]

[a] Measured from PG. [b] Lifespan: 2 days.

compared to *t*BuClOAc. In addition, $T_{gel-sol}$ increased as the amount of acid decreased in both gel systems. This trend is likely due to the presence of residual precursor gelators in samples with lower acid content, which have higher melting points than the individual gelators and may reinforce the gel network, thereby raising the transition temperature.

NMR studies

Initial state. Nuclear magnetic resonance (NMR) spectroscopy was performed on solutions of vacuum-dried xerogels (prepared with 1.0 eq. of acid) to assess the gelation mechanism and to compare it with previously published systems[27,28] (Fig. 2 and Fig. S22, SI). Two amide signals, appearing at approximately 9 ppm, indicate the presence of two different gelators (Fig. 2a; **2a** : **2b** with a ratio of 0.50 : 1.00, Fig. 2b; **1a** : **1b** with a ratio of 1.00 : 0.26). Their presence in the gel system is further corroborated by a singlet at ~1.3 ppm corresponding to the *tert*-butyl group of gelator **1a** or **2a** and a peak at 8.05 ppm assigned to the protonated NH_2 (NH_3^+). The ratio of gelators varies dynamically within the systems. This is evident from the NMR spectra measured on different gel batches on the day of gel formation, in which the gelator ratio differs among batches (Fig. S28, SI).

In our previous studies, the formation of *t*BuOH as a result of solvent decomposition was shown to be crucial for the gelation mechanism and gel stability, specifically through the hydrolysis/esterification cycle, as well as for the subsequent collapse of the gel.[27,28]

Although gel systems are dried under vacuum, their drying may be more or less incomplete, as solvent peaks are clearly visible in gel NMR spectra (S4, SI). Therefore, for example, *t*BuOH should also be detectable in the NMR spectra. To our surprise, no *t*BuOH was observed in the *t*BuClOAc samples. To determine whether *t*BuOH forms, we first tested whether the solvent alone undergoes acid-catalysed decomposition. The reaction was monitored by NMR spectroscopy, with spectra measured before acid addition and at regular time intervals thereafter. Solvent decomposition was clearly observed, confirming the release of the tBu^+ cation. However, *t*BuOH was not detected in either the xerogels or the solvent (S7, SI). The same test was also performed using *t*BuOMe as the solvent, which showed solvent decomposition. Interestingly, although *t*BuOH was not detected in the solvent spectra, a broad peak at ~6.75 ppm (Fig. 2b), corresponding to the hydroxyl group of *t*BuOH, was detected in the gel samples prepared in *t*BuOMe. This suggests that, although *t*BuOH may also form in solution, its concentration is likely below the detection limit, or that the hydroxyl resonance is broadened beyond observation due to rapid proton exchange. In the gel state, however, supramolecular confinement may stabilize and enrich *t*BuOH, giving rise to the detectable broad resonance at ~6.75 ppm in the case of *t*BuOMe systems.

***t*BuOMe, the solvent with two potential leaving groups.** Depending on the initial precursor gelator, the formation of a third gelator, either PhePheOMe (**1c**) or LeuPheOMe (**2c**), was identified by additional peaks in the NH region (~9 ppm; Fig. S20 and S22, SI) and at ~3.60 ppm, corresponding to the methyl group (Me) of the ester. During hydrolysis of the primary solvent, *t*BuOMe, two secondary solvents, *t*BuOH and methanol (MeOH), are generated. Consequently, MeOH can also participate in the esterification reaction, leading to the incorporation of the Me-group (Scheme 2b). The presence of MeOH is further supported by the NMR spectra of most xerogels (S4.3 and S4.4, SI), where a singlet at ~3.16 ppm corresponds to the methyl group of MeOH. Additionally, the *t*Bu-group of *t*BuOH appears at ~1.10 ppm, along with a broad, shifting peak attributed to the hydroxyl group of either alcohol. In both gel systems, the presence of the third gelator is also confirmed by high-resolution mass spectrometry (HR-MS) (S4.3 and S4.4, SI).

It should be noted that the formation of the third gelator occurs somewhat randomly, mirroring the variability observed in the ratios of the other two gelators. The use of a solvent capable of generating two leaving groups may partially explain this variability in gelation outcomes and the prolonged gelation time. These findings suggest that solvents with multiple potential leaving groups provide greater tunability in solvent-induced gelation systems and indicate that the leaving groups of the precursor gelator and the solvent do not necessarily need to match.

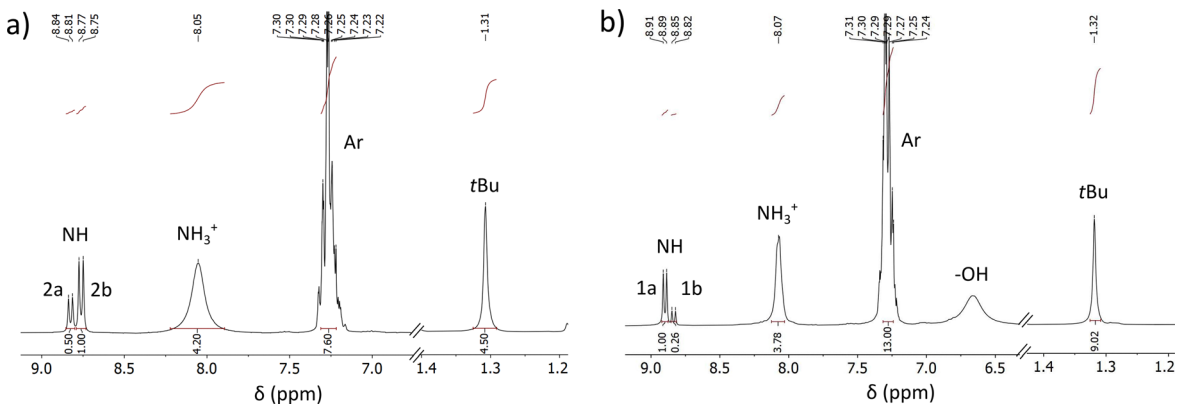

Fig. 2 ^{1}H NMR spectra of (a) gel system **II** in *t*BuClOAc and (b) gel system **I** in *t*BuOMe. In all samples 1.0 eq. of acid was used.

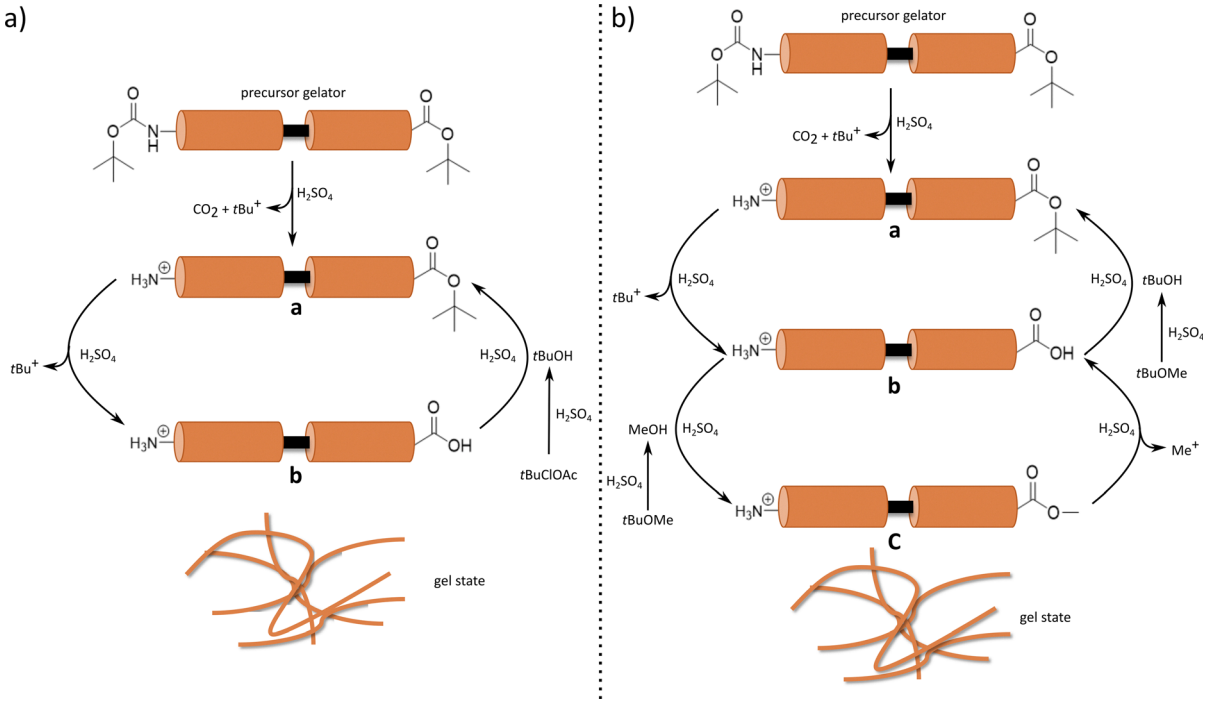

Scheme 2 Proposed gelation mechanism in different solvent systems: (a) *t*BuClOAc and (b) *t*BuOMe.

The effect of acid concentration on gel systems. The effect of acid concentration on the gels was investigated by NMR spectroscopy. At lower acid amounts (0.5–0.18 eq.), two additional doublets around 8 ppm and 7 ppm, along with a singlet at 1.3 ppm, were observed. These signals correspond to the amide proton (NH*) and the Boc-group (Boc*) of precursor gelator **1** or **2** (Fig. 3), indicating incomplete deprotection at low acid concentrations. In *t*BuOMe, the NMR spectra of xerogels formed with 0.5 and 0.18 eq. of acid clearly show these additional peaks (Fig. S24 and S26, SI).

In contrast, gels formed in *t*BuClOAc at the same acid concentrations do not consistently display these peaks (Fig. S6, S8, S12 and S14, SI). This difference arises from variations in the initial pH of the precursor gelator solutions; for example, at the lower final pH (after acid addition), Boc deprotection is more complete. Nevertheless, more sensitive HR-MS can still detect residual precursor gelators in the systems, even when NMR does not clearly reveal their presence (S4.1 and S4.2, SI).

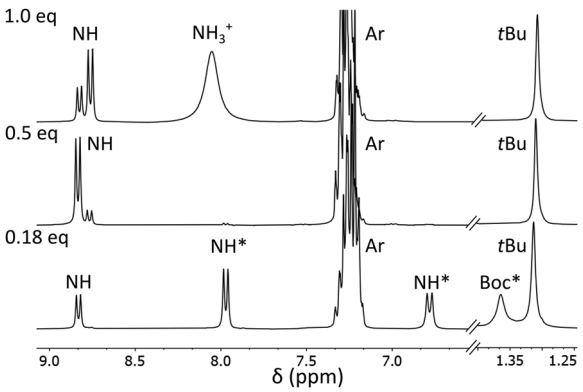

Fig. 3 ^{1}H NMR spectra of gel system **I** in *t*BuOMe with different acid equivalents.

Assessing the secondary structure of gels by ATR-FTIR

Infrared (IR) spectroscopy of xerogel samples was conducted to assess the self-assembly and supramolecular interactions in the corresponding gels (Fig. 4). Particular attention was given to the amide I region (1700–1600 cm^{-1}), where absorption bands arise primarily from C=O stretching vibrations with minor contributions from N–H plane bending. Vibrations in this region are sensitive to C=O···H–N hydrogen bond formation and are directly influenced by the resulting secondary structure.[29,30]

In gel system **I** with *t*BuClOAc and 0.5 eq. of acid (Fig. 4a, red solid line), a single band at 1666 cm^{-1}, corresponding to a β-sheet structure, is observed. In contrast, at 0.18 eq. of acid (solid blue), two weak bands attributed to β-sheet structures appear at 1681 cm^{-1} and 1667 cm^{-1}, together with a peak at 1654 cm^{-1} indicative of a helical-like assembly. For the xerogels of gel system **I** prepared from *t*BuOMe (dotted lines), both helical-like and β-sheet structures are present for all acid concentrations. The helical-like band consistently appears around 1650 cm^{-1}, regardless of acid equivalency. However, the β-sheet bands show minor variations as the acid equivalency changes. The band appears broader at higher acid concentrations (1.0 and 0.5 eq.) compared to the lowest acid concentration (0.18 eq.), and their positions shift irregularly with acid concentration (1.0 eq.: 1673 cm^{-1}; 0.5 eq.: 1666 cm^{-1} and 0.18 eq.: 1684 cm^{-1}).

For gel system **II**, the secondary structures of xerogels in *t*BuClOAc vary with acid concentration. The xerogel formed

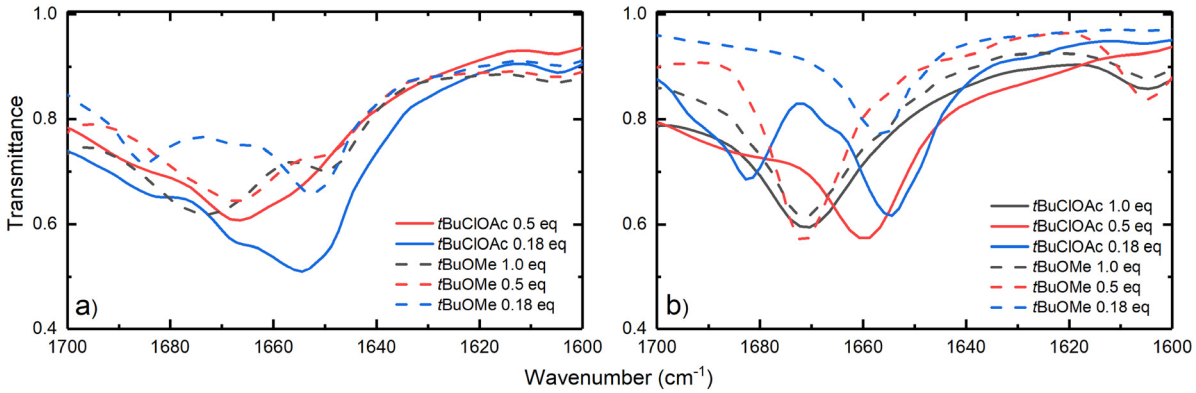

Fig. 4 ATR-FTIR spectra showing the amide I region (1600–1700 cm^{-1}) of (a) gel system **I** and (b) gel system **II** in *t*BuClOAc (solid line) and *t*BuOMe (dotted line) at different acid equivalents. The spectrum of the sample formed by 1.0 eq. of acid in *t*BuClOAc could not be measured as gelation was not observed.

with 1.0 eq. of acid (solid black, Fig. 4b) shows a broad band at 1671 cm^{-1} associated with β-sheet formation. At 0.5 eq. of acid (solid red), only a broad peak (1660 cm^{-1}) related to a helical-like structure is observed. In the sample prepared with the lowest acid content (0.18 eq.), bands corresponding to both β-sheet (1684 cm^{-1}) and helical-like structures (1654 cm^{-1}) appear. For xerogels of gel system **II** prepared with *t*BuOMe, only a peak corresponding to a β-sheet around 1671 cm^{-1} is observed at higher acid concentrations (1.0 and 0.5 eq.). In contrast, at 0.18 eq. the dominant structure is helical, as indicated by a peak at 1657 cm^{-1}.

As expected from the literature,[31–33] β-sheet structures are found in these xerogels in both solvents. The position and number of β-sheet bands vary depending on the type of β-sheet (parallel or antiparallel), the number of strands, and the degree of twisting within the sheets.[29] Notably, short helices or helical-like structures with fewer than six residues typically do not exhibit the characteristic α-helix absorption. However, several bands can still arise in the amide I region due to shorter helical-like conformations.[29] In our previous studies, helical-like structures were frequently observed.[27,28] In addition, detailed investigations of a related gel system revealed a distinct helical-like band, although the β-sheet remained as the dominant nanoscale structure.[34] The helical-like features observed in the current study are likely due to the coexistence of multiple gelators, including the precursor gelator, and their respective distribution within the samples. This also accounts for the variation in secondary structure peaks, particularly in response to acid concentration.

Morphological features

To investigate the effects of solvent and the type of precursor gelator on the morphology of the gel network, the gel systems were imaged using transmission electron microscopy (TEM, Fig. 5 and Fig. S40a–c, SI), atomic force microscopy (AFM, Fig. S40d, SI) and scanning electron microscopy (SEM, Fig. S41, SI) Imaging was performed on gels prepared with 0.5 eq. of acid and diluted before drying at room temperature (standard protocol, S1, SI). However, the exceptions are systems

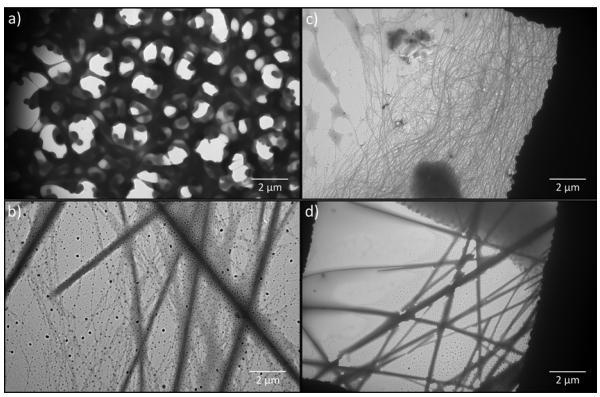

Fig. 5 TEM images of 0.5 eq. of gel systems in *t*BuClOAc: (a) gel system **I** and (b) gel system **II**, and in *t*BuOMe: (c) gel system **I** and (d) gel system **II**. Scale bars are shown in the image.

imaged with SEM that were vacuum-dried, and the samples were prepared by dipping the grid directly into the gel (S1, SI).

In the case of gel system **I** in *t*BuClOAc, the standard protocol was modified because the gel matrix collapsed under the standard conditions (Fig. S40a, SI). To address this issue, the gel was transferred directly onto the chip and allowed to dry at room temperature. This approach resulted in a scaffold-like structure composed of shorter, flattened ribbons connected to wider, flatter bundles, forming a porous network (Fig. 5a), as confirmed by TEM. A similar porous network can be observed in the TEM image (Fig. S41a_2, SI) of the 0.18 eq. system. Furthermore, a distinct ribbon structure is observed (Fig. S41a_1 and a_2, SI).

Using the standard sample-preparation protocol, gel system **I** in *t*BuOMe (Fig. 5c) produced a dense, fibrous network of thin, long, entangled fibres. Additionally, needle-like structures were observed (Fig. S40c, SI). Also, TEM images (Fig. S41b_1, b_2, SI) show similar needle-like structures that begin to intertwine together to form a larger bundle-like structure. In gel system **II** in *t*BuClOAc (Fig. 5b), long, straight fibres were observed alongside thin, intertwined individual fibres. Furthermore, long, narrow, separate, and breached single fibres as well as

flat ribbons were present (Fig. S40b, SI). Gel system **II** in *t*BuOMe exhibited elongated, straight fibres (Fig. 5d), together with bundles and flat ribbons (Fig. S40d, SI).

The morphologies of gel system **II** were broadly similar across solvents, except that in the *t*BuClOAc system (Fig. 5b), single entangled fibres were also observed, a feature likewise characteristic of gel system **I** in *t*BuOMe (Fig. 5c). The two gel system **I** samples cannot be directly compared due to differences in sample preparation. However, the divergent behaviour during preparation suggests inherent differences between the systems. Indeed, Phe-derivatives are well known as self-assembling molecules.[31,35] Even small changes in molecular structure or environmental conditions can lead to significant morphological differences.[36] In the present case, the environment is influenced by the distribution of active gelators (which cannot be precisely controlled), acid content, and the choice of solvent, all of which contribute to the resulting gel morphology.

Conclusions

This study demonstrates that the unique solvent-induced gelation mechanism can be adapted to different solvent environments and that the acid concentration affects the gelation process. The gelation time, final outcome, and supramolecular structure of the resulting materials can be tuned by varying both the solvent and the acid concentration. In *t*BuClOAc, the gelation time remained constant regardless of the acid amount, whereas in *t*BuOMe, the gelation time increased as the acid concentration decreased. Acid concentration also determined the outcome of gelation in *t*BuOMe, influencing whether a self-supporting or partial gel was obtained, and affecting the efficiency of precursor gelator-to-gelator conversion. These effects were consistent across both dipeptide systems, highlighting the critical role of solvent and acid, independent of gelator structure.

Switching from the previously studied *t*BuOAc to *t*BuClOAc and *t*BuOMe impacted gel stability and transient behaviour, with the new systems producing stable gels to date. Notably, *t*BuOMe acted as a ''solvent with two leaving groups'' as evidenced by NMR spectroscopy. These findings show that solvent-induced systems are adaptable and that the leaving groups in the solvent and in the precursor gelator do not necessarily need to match. However, the presence of multiple leaving groups may prolong gelation time and favour the formation of partial gels.

Both gel systems exhibited diverse supramolecular structures in the solvents studied. β-sheet structures were the dominant secondary motif in ATR-FTIR spectra. In *t*BuClOAc, helical-like structures emerged at lower acid concentrations, independent of the precursor gelator. By contrast, secondary structure formation in *t*BuOMe was less systematic, likely due to the dual leaving groups. Notably, *t*BuClOAc exhibited more pronounced structural changes with varying acid concentrations compared to *t*BuOMe.

Overall, this study provides new insights into the tunability of solvent-induced gelation systems. Deliberate manipulation of ester groups in precursor gelators, together with variation in solvent leaving groups, offers promising strategies for tailoring gelation behaviour, material stability, and mechanical properties. Furthermore, the scaffold-like architectures suggest potential applications in areas such as cell culture scaffolds or drug delivery platforms.

Experimental

Synthesis of precursor gelators and the corresponding active gelators

Compounds **1–3**, **1a and 2a** were synthesised according to previous protocols.[28] As an exception, NaCl was used in the separation of water phases to prevent suspension formation. In addition, two water washes were added at the end of the purification process (S2.1, SI).

General protocol for the synthesis of 2c. The Boc-protected dipeptide methyl ester (1.0 eq.) was suspended in DCM at a concentration of 0.2 M. TFA (10 eq.) was added dropwise to the solution at room temperature, and the reaction mixture was left to stir under a N_2 atmosphere overnight. DCM was added to dilute the reaction mixture before evaporating the solvents under vacuum. DCM was added to the obtained residue (3×), and the mixture was further evaporated.

Gelation protocol

The precursor gelator (**1**: 23.5 mg, 0.05 M; or **2**: 21.7 mg, 0.05 M) was suspended in the corresponding organic solvent (1 mL) and sonicated until dissolution or a fine suspension formed, before adding concentrated H_2SO_4 (1.0, 0.5, or 0.18 eq.). The mixture was gently swirled and left at room temperature for gelation to occur. Gelation was confirmed by the vial-inversion test.

Author contributions

H. R.: conceptualisation, formal analysis, investigation, validation, visualisation, writing – original draft, review and editing. E. D. S.: conceptualisation, supervision, writing – review and editing. R. C.: conceptualisation, writing – review and editing. M. N.: supervision, validation, writing – review and editing.

Conflicts of interest

There are no conflicts to declare.

Data availability

The data supporting this article are included as part of the supplementary information (SI). Supplementary information: synthesis and characterisation of **2c** and **3**. Gelation experiments and NMR spectra of gels and degraded solvents, ATR-FTIR spectra of xerogels, AFM, TEM and SEM images. See DOI: https://doi.org/10.1039/d5cp03810c.

The original files are available from the corresponding author upon request.

Acknowledgements

E. D. S. acknowledges the Jane and Aatos Erkko Foundation for supporting the work. Dr Andreas Johansson is thanked for operating the TEM and SEM, and MSc Veera Nikkola, and MSc Jenni Rive for preliminary gelation tests.

References

1 P. Terech and R. G. Weiss, *Chem. Rev.*, 1997, **97**, 3133–3160.
2 G. Yu, X. Yan, C. Han and F. Huang, *Chem. Soc. Rev.*, 2013, **42**, 6697–6722.
3 D. Giuri, F. Cenciarelli and C. Tomasini, *J. Pept. Sci.*, 2024, **30**, e3643.
4 S. Fleming and R. V. Ulijn, *Chem. Soc. Rev.*, 2014, **43**, 8150–8177.
5 T. Das, M. Häring, D. Haldar and D. Díaz Díaz, *Biomater. Sci.*, 2018, **6**, 38–59.
6 J. Wang, K. Liu, R. Xing and X. Yan, *Chem. Soc. Rev.*, 2016, **45**, 5589–5604.
7 T. Li, X.-M. Lu, M.-R. Zhang, K. Hu and Z. Li, *Bioactive Mater.*, 2022, **11**, 268–282.
8 M. A. Kuzina, D. D. Kartsev, A. V. Stratonovich and P. A. Levkin, *Adv. Funct. Mater.*, 2023, **33**, 2301421.
9 J. Kim, T. H. Han, Y. Kim, J. S. Park, J. Choi, D. G. Churchill, S. O. Kim and H. Ihee, *Adv. Mater.*, 2010, **22**, 583–587.
10 Y. Wang, W. Qi, R. Huang, X. Yang, M. Wang, R. Su and Z. He, *J. Am. Chem. Soc.*, 2015, **137**, 7869–7880.
11 C. Zhao, Y. Wang, B. Shi, M. Li, W. Yan and H. Yang, *Langmuir*, 2022, **38**, 7965–7975.
12 J. Boekhoven, A. M. Brizard, K. N. K. Kowlgi, G. J. M. Koper, R. Eelkema and J. H. van Esch, *Angew. Chem.*, 2010, **122**, 4935–4938.
13 S. A. P. Van Rossum, M. Tena-Solsona, J. H. Van Esch, R. Eelkema and J. Boekhoven, *Chem. Soc. Rev.*, 2017, **46**, 5519–5535.
14 B. Rieß, C. Wanzke, M. Tena-Solsona, R. K. Grötsch, C. Maity and J. Boekhoven, *Soft Matter*, 2018, **14**, 4852–4859.
15 M. Fialkowski, K. J. M. Bishop, R. Klajn, S. K. Smoukov, C. J. Campbell and B. A. Grzybowski, *J. Phys. Chem. B*, 2006, **110**, 2482–2496.
16 G. Ragazzon and L. J. Prins, *Nat. Nanotechnol.*, 2018, **13**, 882–889.
17 B. Rieß and J. Boekhoven, *ChemNanoMat*, 2018, **4**, 710–719.
18 L. Zeng, X. Lin, P. Li, F.-Q. Liu, H. Guo and W.-H. Li, *Prog. Org. Coat.*, 2021, **159**, 106417.
19 J. Raeburn, C. Mendoza-Cuenca, B. N. Cattoz, M. A. Little, A. E. Terry, A. Zamith Cardoso, P. C. Griffiths and D. J. Adams, *Soft Matter*, 2015, **11**, 927–935.
20 G. Zhu and J. S. Dordick, *Chem. Mater.*, 2006, **18**, 5988–5995.
21 S. Wu, J. Gao, T. J. Emge and M. A. Rogers, *Soft Matter*, 2013, **9**, 5942–5950.
22 D. M. Zurcher and A. J. McNeil, *J. Org. Chem.*, 2015, **80**, 2473–2478.
23 Y. Lan, M. G. Corradini, R. G. Weiss, S. R. Raghavan and M. A. Rogers, *Chem. Soc. Rev.*, 2015, **44**, 6035–6058.
24 E. R. Draper and D. J. Adams, *Chem*, 2017, **3**, 390–410.
25 M. L. Muro-Small, J. Chen and A. J. McNeil, *Langmuir*, 2011, **27**, 13248–13253.
26 P. Zhu, X. Yan, Y. Su, Y. Yang and J. Li, *Chem. – Eur. J.*, 2010, **16**, 3176–3183.
27 R. Chevigny, J. Schirmer, C. C. Piras, A. Johansson, E. Kalenius, D. K. Smith, M. Pettersson, E. D. Sitsanidis and M. Nissinen, *Chem. Commun.*, 2021, **57**, 10375–10378.
28 R. Chevigny, H. Rahkola, E. D. Sitsanidis, E. Korhonen, J. R. Hiscock, M. Pettersson and M. Nissinen, *Chem. Mater.*, 2024, **36**, 407–416.
29 A. Barth, *Biochim. Biophys. Acta, Bioenerg.*, 2007, **1767**, 1073–1101.
30 J. Kong and S. Yu, *Acta Biochim. Biophys. Sin.*, 2007, **39**, 549–559.
31 X. Yan, P. Zhu and J. Li, *Chem. Soc. Rev.*, 2010, **39**, 1877–1890.
32 X. Yan, Y. Cui, Q. He, K. Wang and J. Li, *Chem. Mater.*, 2008, **20**, 1522–1526.
33 S. Marchesan, L. Waddington, C. D. Easton, D. A. Winkler, L. Goodall, J. Forsythe and P. G. Hartley, *Nanoscale*, 2012, **4**, 6752–6760.
34 R. Chevigny, E. D. Sitsanidis, J. Schirmer, E. Hulkko, P. Myllyperkiö, M. Nissinen and M. Pettersson, *Chem. – Eur. J.*, 2023, **29**, e202300155.
35 P. Sahandi Zangabad, Z. Abousalman Rezvani, Z. Tong, L. Esser, R. B. Vasani and N. H. Voelcker, *ACS Appl. Bio Mater.*, 2023, **6**, 3532–3554.
36 S. Marchesan, A. V. Vargiu and K. E. Styan, *Molecules*, 2015, **20**, 19775–19788.